

**Excitation function of the  $^{60}\text{Ni}(p,\gamma)^{61}\text{Cu}$  reaction from threshold to 16 MeV**M. S. Uddin,<sup>1,2,\*</sup> S. Sudár,<sup>3</sup> I. Spahn,<sup>2</sup> M. A. Shariff,<sup>1</sup> and S. M. Qaim<sup>2</sup><sup>1</sup>*Tandem Accelerator Facilities, Institute of Nuclear Science and Technology, Atomic Energy Research Establishment, Savar, Dhaka, Bangladesh*<sup>2</sup>*Institut für Neurowissenschaften und Medizin, INM-5:Nuklearchemie, Forschungszentrum Jülich, D-52425 Jülich, Germany*<sup>3</sup>*Institute of Experimental Physics, Debrecen University, H-4001 Debrecen, Hungary*

(Received 2 December 2015; revised manuscript received 18 February 2016; published 12 April 2016)

Excitation function of the reaction  $^{60}\text{Ni}(p,\gamma)^{61}\text{Cu}$  was measured via the activation technique in the energy range of 1.3–16.0 MeV using a low-energy accelerator and a small cyclotron. The results are comparable to those previously obtained via prompt  $\gamma$  counting. In addition excitation functions of the more common competing  $^{60}\text{Ni}(p,n)^{60}\text{Cu}$  and  $^{60}\text{Ni}(p,\alpha)^{57}\text{Co}$  reactions were also measured. Theoretical calculations on proton-induced reactions on  $^{60}\text{Ni}$  were performed using the nuclear model code TALYS. The results suggest that near the threshold of the reaction the compound nucleus mechanism dominates. Thereafter the contribution of direct interactions becomes rather strong, especially between 4 and 6 MeV, i.e., just below the threshold of the  $^{60}\text{Ni}(p,n)^{60}\text{Cu}$  reaction. The cross section at the maximum of the excitation function of each of the three reactions, namely,  $^{60}\text{Ni}(p,\gamma)^{61}\text{Cu}$ ,  $^{60}\text{Ni}(p,n)^{60}\text{Cu}$ , and  $^{60}\text{Ni}(p,\alpha)^{57}\text{Co}$ , amounts to 2, 320, and 85 mb, respectively. The  $(p,n)$  reaction is thus the most commonly occurring process, and the  $(p,\gamma)$  reaction is the weakest, possibly due to higher probability of particle emission than  $\gamma$ -ray emission from the highly excited intermediate nucleus  $^{61}\text{Cu}$  formed in the interaction of a proton with the target nucleus  $^{60}\text{Ni}$ .

DOI: [10.1103/PhysRevC.93.044606](https://doi.org/10.1103/PhysRevC.93.044606)**I. INTRODUCTION**

The radiative capture of slow neutrons, i.e., the  $(n,\gamma)$  process, is a very special case because it can occur at the lowest neutron energies and, in the eV energy range, it preferentially populates high-lying closely spaced levels of the intermediate nucleus, resulting in strong resonances. For energies beyond 500 eV, however, the  $(n,\gamma)$  cross section is considerably reduced due to the onset of competing reaction channels. In contrast, due to the Coulomb barrier effect the radiative capture of a proton can occur only in the MeV range and, like neutron capture in that energy range, the  $(p,\gamma)$  cross section is low. An experimental study of this reaction seemed worthwhile because the available database for this reaction is rather weak [1–4]. Furthermore, investigation of this nuclear process on light-mass isotopes of a few elements near the reaction threshold is of considerable significance in astrophysics [2,5,6]. In this paper we studied the interactions of protons with  $^{60}\text{Ni}$  with a major emphasis on the  $(p,\gamma)$  reaction.

The  $(p,\gamma)$  reaction cross section can be determined either by registering the prompt  $\gamma$  rays emitted during an irradiation or via the activation technique, i.e., by an assay of the radioactive product. Earlier studies related to the  $(p,\gamma)$  reaction on  $^{60}\text{Ni}$  were performed by investigating the prompt  $\gamma$  rays [7–10], the primary motivation being astrophysics [9,10]. In one study over the energy range of 10–22.5 MeV the activation technique was used [11]. We carried out extensive activation measurements over the energy range of 1.3–16.0 MeV with two motivations: (a) To obtain data in the early rising part of the excitation function of the  $^{60}\text{Ni}(p,\gamma)^{61}\text{Cu}$  reaction

by an independent technique. Although the resolution of the activation data is not comparable to that of the data obtained by prompt  $\gamma$ -ray counting, for the formation of the product nucleus, the activation data are very relevant. (b) To test contemporary nuclear model calculations for this reaction in the low-energy region. During this work some additional information was gained on the more common competing  $^{60}\text{Ni}(p,n)^{60}\text{Cu}$  and  $^{60}\text{Ni}(p,\alpha)^{57}\text{Co}$  reactions for which some data were available in the literature. We report them here to show the predictive power of model calculations for the more common nuclear reactions and to discuss the relative contributions of the three processes studied, viz.  $(p,\gamma)$ ,  $(p,n)$  and  $(p,\alpha)$  reactions.

**II. EXPERIMENTS**

Excitation functions of the proton-induced reactions on  $^{60}\text{Ni}$  were measured using the stacked-foil activation technique. The work involved irradiation of two types of nickel samples;  $^{nat}\text{Ni}$  foils (Goodfellow: purity 99.95%; 10- and 25- $\mu\text{m}$  thicknesses) and enriched  $^{60}\text{Ni}$  sediments (isotopic enrichment 99.9%, chemical purity 99.79%; 4 to 5  $\text{mg}/\text{cm}^2$  of  $^{60}\text{Ni}$  on 50- $\mu\text{m}$ -thick Al backing), and identification of the product radionuclides. Several stacks consisting of either  $^{nat}\text{Ni}$  or  $^{60}\text{Ni}$ , each with Cu-monitor foils, were irradiated with protons of primary energy of  $5.02 \pm 0.03$  MeV at the 3-MV tandem accelerator (High Voltage Engineering Europa B.V.) of the Atomic Energy Research Establishment, Savar, Dhaka, Bangladesh and with  $16.0 \pm 0.2$ -MeV protons at the Baby Cyclotron BC1710 of the Forschungszentrum Jülich, Germany. Details related to sample preparation, beam characterization, experimental arrangements, and irradiations in the case of BC1710 have been recently described in Ref. [12], and those related to the tandem accelerator have

\*Author to whom correspondence should be addressed: md.shuzauddin@yahoo.com

been described in Ref. [13]. The beam current and irradiation time were selected to have enough activities of the investigated product radionuclides.

The proton beam flux reaching the target was measured by charge integration. It was also determined using the  ${}^{\text{nat}}\text{Cu}(p,x){}^{62}\text{Zn}$ ,  ${}^{\text{nat}}\text{Cu}(p,x){}^{63}\text{Zn}$ , and  ${}^{\text{nat}}\text{Cu}(p,x){}^{65}\text{Zn}$  monitor reactions induced in the Cu foil mounted in the front of a stack. The cross sections of those monitor reactions were taken from an evaluated data file [14].

The beam energy degradation along the stack was calculated using the computer program STACK based on the energy-range relation described by Williamson *et al.* [15]. The primary proton energy was checked by a comparison of the normalized activities of two different threshold reaction products induced in a monitor foil [16], e.g.,  ${}^{63}\text{Zn}/{}^{65}\text{Zn}$  and  ${}^{62}\text{Zn}/{}^{65}\text{Zn}$  in the case of the Cu foil. Starting with the primary particle energy incident on the front foil of the stack, the particle energy ( $\bar{E}$ ) effective at each sample was obtained taking a mean of the ingoing and outgoing particle energies. This approximation for the effective particle energy is valid only if the foil is thin or the excitation function of the investigated reaction is approximately constant over the energy range covered by the foil. Since in our paper the foils were not all thin, a correction in energy, similar to one described earlier [17], was applied.

In general, the measured mean cross section ( $\bar{\sigma}$ ) can be expressed in the following form:

$$\bar{\sigma} = \frac{1}{d} \int_0^d \sigma[E(x)] dx,$$

where  $d$  and  $\sigma[E(x)]$  are the thickness of the foil and the cross section of the investigated reaction as a function of the energy in the foil, respectively. The equation  $E(x) = E_{\text{in}} - \int_0^x (\frac{dE}{dx}) dx$  describes the variation of the energy inside the foil, where  $E_{\text{in},x}$ ,  $(\frac{dE}{dx})$  are the incident energy, the distance from the surface in the beam direction, and the stopping power, respectively. Generally,  $\bar{\sigma}$  is not equal to  $\sigma(\bar{E})$ , but there exists an energy  $\hat{E}$  for which  $\bar{\sigma} = \sigma(\hat{E})$  and  $E_{\text{out}} \leq \hat{E} \leq E_{\text{in}}$ .  $\hat{E}$  was estimated by using the excitation functions of the investigated reactions derived from the model calculations in the following way: A value  $\bar{\sigma}_{\text{th}}$  was derived from the calculated cross sections, and  $\hat{E}$  was interpolated to fulfill the  $\bar{\sigma}_{\text{th}} = \sigma_{\text{th}}(\hat{E})$  equation. Only the shape of the excitation function used is similar to the theoretical one. The numerical integration and the inverse interpolation are included into our energy degradation calculation program which calculates average exit energy of the particles from the foils in the stack. The inverse interpolation may cause difficulty when the excitation function is not monotonic in the energy range covered by one foil, i.e., if there is a sharp resonance in this energy range. In our case the theoretical excitation function does not have resonances, therefore the inverse interpolation is unambiguous, and the experimental data do not indicate resonances with the energy resolution of the applied experimental method. During the numerical integration one foil (10  $\mu\text{m}$ ) is divided in about 100 parts, which give enough accuracy to the calculation.

This method and some other methods [cf. 18] gave significant differences, compared with the usual simple estimation method for obtaining the mean energy, only near the reaction

threshold. Theoretical calculations are available for a wide range of reactions [cf. 19]; the use of this formula could thus improve the reliability of the experimental data.

The radioactivity of a reaction product in the activated foil was measured nondestructively using HPGe-detector  $\gamma$ -ray spectrometry. Each sample was counted several times to check the half-life of the activation product. The efficiency versus energy curve of the  $\gamma$ -ray detector was determined using the standard point sources  ${}^{57}\text{Co}$ ,  ${}^{60}\text{Co}$ ,  ${}^{133}\text{Ba}$ ,  ${}^{137}\text{Cs}$ , and  ${}^{152}\text{Eu}$ , traceable to Physikalisch Technische Bundesanstalt (PTB) Braunschweig, Germany. The decay data of the investigated radionuclides were taken from the Lund University/Lawrence Berkeley National Laboratory database [20].

The work with the enriched  ${}^{60}\text{Ni}$  target was straightforward since all products could be assigned to specific reactions. In the case of the  ${}^{\text{nat}}\text{Ni}$  target, however, some corrections had to be applied. The radionuclide  ${}^{61}\text{Cu}$  was produced below 3 MeV only via the  ${}^{60}\text{Ni}(p,\gamma)$  reaction. At higher energies, the reactions  ${}^{61}\text{Ni}(p,n)$  and  ${}^{62}\text{Ni}(p,2n)$  also contributed. Recently, Aslam and Qaim [21] published recommended data for the  ${}^{61}\text{Ni}(p,n){}^{60}\text{Cu}$  reaction after a critical analysis of all experimental data. Those data were utilized to determine the contribution of the  $(p,n)$  reaction to  ${}^{61}\text{Cu}$  formation. The  ${}^{61}\text{Cu}$  activity due to the  ${}^{62}\text{Ni}(p,2n)$  reaction was estimated from the data of Piel *et al.* [16], which were measured by the proton interaction on the enriched  ${}^{62}\text{Ni}$  target. The contributions of the two reactions, i.e.  $(p,n)$  and  $(p,2n)$ , from their corresponding threshold energies to 16 MeV, were subtracted from the total measured activity to determine the  ${}^{61}\text{Cu}$  activity produced only via the  ${}^{60}\text{Ni}(p,\gamma)$  reaction. In contrast, the radionuclide  ${}^{60}\text{Cu}$  is formed mostly via the  ${}^{60}\text{Ni}(p,n)$  reaction with some contribution from the  ${}^{61}\text{Ni}(p,2n)$  reaction. However, due to the low isotopic abundance of  ${}^{61}\text{Ni}$  and the low cross section below 16 MeV the contribution of the  ${}^{61}\text{Ni}(p,2n)$  reaction to the production of  ${}^{60}\text{Cu}$  is rather small. Because of the threshold energy of 14.95 MeV, only in a few targets in the front of the stack was a small correction undertaken by using the cross-sectional data of Szelecsényi *et al.* [22].

The radionuclide  ${}^{57}\text{Co}$  is produced through the reactions  ${}^{60}\text{Ni}(p,\alpha){}^{57}\text{Co}$  and  ${}^{58}\text{Ni}(p,2p){}^{57}\text{Co}$  and in the decay of  ${}^{57}\text{Ni}$ . For applying corrections for the reaction  ${}^{58}\text{Ni}(p,2p){}^{57}\text{Co}$ , averages of the values available in the literature [23–25] were used, and the International Atomic Energy Agency recommended values [14] were applied for the  ${}^{\text{nat}}\text{Ni}(p,x){}^{57}\text{Ni}$  reaction.

The count rate of each radionuclide produced in a single process was extrapolated to the end of the bombardment, and it was converted to a decay rate by applying the usual corrections, such as the intensity of the  $\gamma$  ray used, the efficiency of the detector, etc. From the decay rate and proton flux determined via the monitor reaction, the nuclear reaction cross section was calculated using the well-known activation equation. The overall uncertainty in the cross section was obtained by a quadratic summing of the individual uncertainties involved in all parameters needed to calculate the cross section. The uncertainty of each cross-sectional value includes individual uncertainties, e.g., counting statistics (0.2%–10%), spectrum analysis (0.5%), efficiency of the detector (4%), half-life of the product (0.1%–1.6%),  $\gamma$ -ray intensity (0.2%–6%),

TABLE I. Measured cross sections of the  $^{60}\text{Ni}(p,\gamma)^{61}\text{Cu}$  reaction using the 3-MV tandem accelerator.

Proton energy <sup>a</sup> (MeV)	Cross section (mb)
$3.94 \pm 0.26$	$1.17 \pm 0.12$
$3.61 \pm 0.29$	$1.33 \pm 0.13$
$3.41 \pm 0.29$	$1.13 \pm 0.14$
$2.98 \pm 0.30$	$1.04 \pm 0.13$
$2.79 \pm 0.30$	$0.47 \pm 0.06$
$2.48 \pm 0.30$	$0.27 \pm 0.04$
$2.32 \pm 0.39$	$0.26 \pm 0.04$
$2.07 \pm 0.39$	$0.14 \pm 0.02$
$1.64 \pm 0.50$	$0.07 \pm 0.01$
$1.47 \pm 0.50$	$0.04 \pm 0.006$
$1.28 \pm 0.50$	$0.02 \pm 0.003$

<sup>a</sup>The deviation given here describes the energy spread within each foil.

coincidence loss (<0.5%), and monitor reaction cross section (6%–8%). The uncertainty in the number of target nuclei of

<1% was also included. In general, the overall uncertainties associated in measured cross sections are between 7% and 15%. In the case of a few foils in front of a stack, the uncertainty was up to 27% due to the large uncertainty of the adopted cross-sectional value of the  $^{61}\text{Ni}(p,2n)^{60}\text{Cu}$  process.

The 3-MV tandem accelerator delivers the proton with an energy uncertainty of <0.5%. An uncertainty of <1% is associated with the energy of the proton from the BC 1710 Cyclotron. The energy range effective within each foil is given in Tables I and II.

### III. NUCLEAR MODEL CALCULATIONS

Theoretical calculations on proton-induced reactions on  $^{60}\text{Ni}$  were performed using the nuclear model code TALYS (version 1.6), which has been recently developed by Koning *et al.* [26]. The method was recently used in extensive calculations on  $^{192}\text{Os}$  [27] and  $^{100}\text{Mo}$  [28], and the various input parameters, carefully selected, have been described in detail. The spin distribution of the level density was characterized by the ratio of the effective moment of inertia

TABLE II. Measured cross sections of the  $^{60}\text{Ni}(p,\gamma)^{61}\text{Cu}$ ,  $^{60}\text{Ni}(p,n)^{60}\text{Cu}$ , and  $^{60}\text{Ni}(p,\alpha)^{57}\text{Co}$  reactions using the Cyclotron BC 1710.

Proton energy (MeV) <sup>c</sup>	Cross section (mb) <sup>a</sup>			Proton energy (MeV) <sup>c</sup>	Cross section (mb) <sup>b</sup>		
	$^{60}\text{Ni}(p,\gamma)^{61}\text{Cu}$	$^{60}\text{Ni}(p,n)^{60}\text{Cu}$	$^{60}\text{Ni}(p,\alpha)^{57}\text{Co}$		$^{60}\text{Ni}(p,\gamma)^{61}\text{Cu}$	$^{60}\text{Ni}(p,n)^{60}\text{Cu}$	$^{60}\text{Ni}(p,\alpha)^{57}\text{Co}$
$15.9 \pm 0.2$	$0.76 \pm 0.21$	$164 \pm 27$	$85 \pm 9$	$16.0 \pm 0.04$	$0.62 \pm 0.04$	$153 \pm 10$	$79 \pm 6$
$15.7 \pm 0.2$	$0.60 \pm 0.16$	$181 \pm 30$	$81 \pm 8$	$15.6 \pm 0.05$	$0.60 \pm 0.05$	$182 \pm 11$	$68 \pm 5$
$15.5 \pm 0.2$	$0.75 \pm 0.20$	$184 \pm 31$	$79 \pm 8$	$15.1 \pm 0.04$	$0.63 \pm 0.05$	$219 \pm 13$	$77 \pm 6$
$14.9 \pm 0.2$	$0.73 \pm 0.20$	$225 \pm 16$	$78 \pm 8$	$13.4 \pm 0.04$	$0.63 \pm 0.04$	$263 \pm 18$	
$14.2 \pm 0.2$	$0.83 \pm 0.22$	$261 \pm 18$	$76 \pm 8$	$12.0 \pm 0.05$	$0.36 \pm 0.03$		
$13.7 \pm 0.3$	$0.82 \pm 0.07$	$271 \pm 19$	$66 \pm 7$	$9.2 \pm 0.07$	$0.31 \pm 0.02$		
$13.1 \pm 0.3$	$0.78 \pm 0.08$	$301 \pm 20$	$65 \pm 6$	$7.5 \pm 0.08$	$0.56 \pm 0.04$		
$12.2 \pm 0.3$	$0.63 \pm 0.06$	$292 \pm 20$	$59 \pm 6$	$6.6 \pm 0.08$	$0.58 \pm 0.04$		
$11.7 \pm 0.3$	$0.60 \pm 0.05$	$287 \pm 20$	$45 \pm 4$	$5.1 \pm 0.09$	$1.86 \pm 0.14$		
$11.1 \pm 0.3$	$0.64 \pm 0.06$	$288 \pm 20$	$42 \pm 4$	$3.6 \pm 0.14$	$1.22 \pm 0.09$		
$10.0 \pm 0.3$	$0.47 \pm 0.04$	$261 \pm 18$	$27 \pm 2.5$	$3.6 \pm 0.14$	$1.11 \pm 0.08$		
$9.4 \pm 0.4$	$0.33 \pm 0.03$	$262 \pm 18$	$24 \pm 1.7$	$2.7 \pm 0.13$	$0.25 \pm 0.02$		
$8.8 \pm 0.4$	$0.40 \pm 0.04$	$223 \pm 15$	$20 \pm 1.8$				
$8.0 \pm 0.4$	$0.38 \pm 0.04$	$149 \pm 12$	$6.7 \pm 0.5$				
$7.4 \pm 0.4$	$0.55 \pm 0.05$	$66 \pm 5$	$4.7 \pm 0.4$				
$7.1 \pm 0.4$	$0.73 \pm 0.07$	$24 \pm 1.6$	$2.8 \pm 0.2$				
$6.5 \pm 0.4$	$1.36 \pm 0.13$		$0.5 \pm 0.06$				
$6.2 \pm 0.5$	$1.64 \pm 0.15$						
$5.8 \pm 0.5$	$1.76 \pm 0.16$						
$5.5 \pm 0.5$	$1.75 \pm 0.17$						
$5.0 \pm 0.5$	$1.93 \pm 0.19$						
$4.8 \pm 0.5$	$1.86 \pm 0.13$						
$4.3 \pm 0.3$	$1.60 \pm 0.14$						
$4.0 \pm 0.3$	$1.67 \pm 0.15$						
$3.6 \pm 0.3$	$1.64 \pm 0.15$						
$3.3 \pm 0.3$	$1.37 \pm 0.14$						
$3.1 \pm 0.3$	$1.33 \pm 0.13$						
$2.7 \pm 0.3$	$0.55 \pm 0.07$						

<sup>a</sup>The  $^{nat}\text{Ni}$  target was irradiated, and the contribution of interfering reactions was corrected.

<sup>b</sup>The enriched  $^{60}\text{Ni}$  target was irradiated, and no correction for interfering reaction was necessary.

<sup>c</sup>The deviation describes the energy spread within each foil.

to the rigid-body moment of inertia ( $\eta = \Theta_{\text{eff}}/\Theta_{\text{rigid}}$ ). In the present calculations the default parameters were used, except for the number of discrete levels and  $\eta$  values which we chose ourselves. Furthermore, to get a better description of the  $(p, \gamma)$  reaction the direct capture option was switched on.

#### IV. RESULTS AND DISCUSSION

At the tandem accelerator only the  ${}^{60}\text{Ni}(p, \gamma){}^{61}\text{Cu}$  reaction was investigated from 1.28 to 3.94 MeV, and the measured cross sections together with their uncertainties are given in Table I. At the Cyclotron BC 1710, besides the  ${}^{60}\text{Ni}(p, \gamma){}^{61}\text{Cu}$  reaction, the nuclear processes  ${}^{60}\text{Ni}(p, n){}^{60}\text{Cu}$  and  ${}^{60}\text{Ni}(p, \alpha){}^{57}\text{Co}$  were also studied over the whole energy range of reaction threshold to 16 MeV. Most of the measurements were performed using  ${}^{\text{nat}}\text{Ni}$  as a target, and cross sections for the  ${}^{60}\text{Ni}$  target were obtained by applying corrections mentioned above. The results are given in Table II. In addition, many data points were obtained using an enriched  ${}^{60}\text{Ni}$  target where no corrections for interfering reactions were necessary. Those results are given separately in Table II.

The experimentally determined cross sections together with the results of nuclear model calculations for the  ${}^{60}\text{Ni}(p, \gamma){}^{61}\text{Cu}$  reaction are plotted in Fig. 1 as a function of the proton energy. The data available in the literature are also shown in the same figure. As mentioned above, except for the two data points at 10 and 16 MeV measured by Cohen [11] using the activation technique, all the other literature data [7–10] were obtained by assay of prompt  $\gamma$  emission. A comparison of all experimental data suggests that the values by Krivonosov *et al.* [8] are consistent with this paper both in shape and in numerical values. After deconvoluting the effects of energy averaging, the present data showed better consistency with Krivonosov *et al.* below 3 MeV. The present data do not agree with the measurements of Refs. [9,10] in the 2.5–4-MeV energy region where the shapes of the excitation function are also different. Thus, in general our activation measurements give results comparable to those obtained by prompt  $\gamma$  counting.

The results of nuclear model calculations suggest that, starting from the threshold of the reaction up to about 3 MeV, the compound nucleus mechanism dominates. Thereafter the

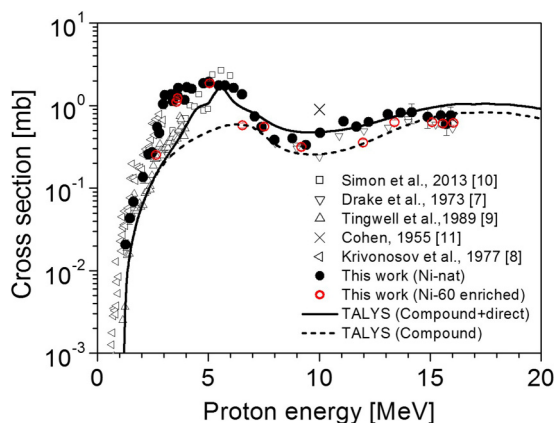


FIG. 1. Measured and calculated excitation function of the  ${}^{60}\text{Ni}(p, \gamma){}^{61}\text{Cu}$  process.

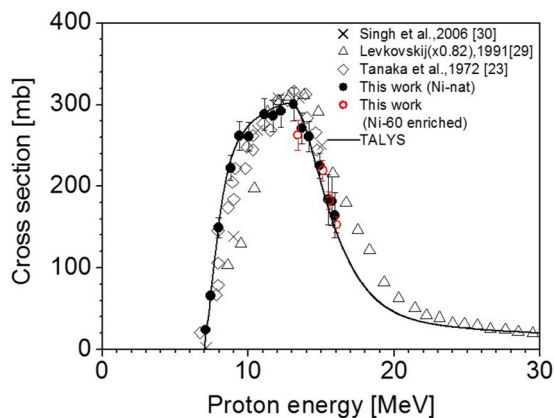


FIG. 2. Measured and calculated excitation function of the  ${}^{60}\text{Ni}(p, n){}^{60}\text{Cu}$  process.

contribution of direct interactions becomes rather strong, especially between 4 and 6 MeV, i.e., just below the threshold of the  ${}^{60}\text{Ni}(p, n){}^{60}\text{Cu}$  reaction. At an energy of 15 MeV, however, the direct contribution amounts to about 30%. In general, the excitation function of the  ${}^{60}\text{Ni}(p, n){}^{60}\text{Cu}$  reaction appears to be reproduced fairly well by the model calculation.

Regarding the two side reactions investigated in this paper, our measured cross sections and the literature experimental data [23,29,30] for the reaction  ${}^{60}\text{Ni}(p, n){}^{60}\text{Cu}$  are shown in Fig. 2. Similarly our and literature [23,24,29] data for the  ${}^{60}\text{Ni}(p, \alpha){}^{57}\text{Co}$  reaction are shown in Fig. 3. It should be mentioned that the data by Levkovskij [29] for both reactions were reduced by a factor of 0.82 as recommended in a recent evaluation [28]. The results of nuclear model calculations are also shown in each figure. Apparently our experimental data are consistent with the literature values over the whole investigated energy range. Furthermore, they are reproduced well by the nuclear model calculations.

The consistency in our results for the  ${}^{60}\text{Ni}(p, \gamma){}^{61}\text{Cu}$  reaction over the overlapping energy region of 2.7–4.0 MeV adds confidence to the experimental techniques used at the two irradiation facilities. This study demonstrates that nuclear

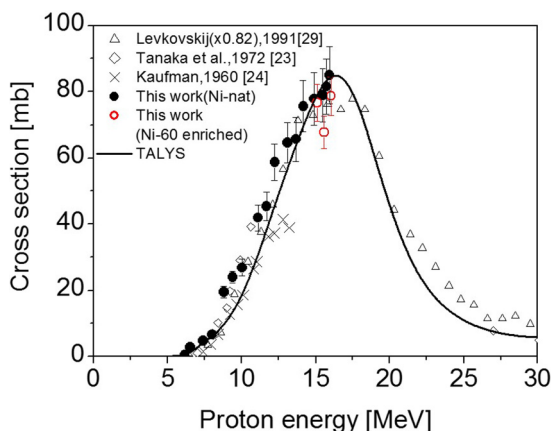


FIG. 3. Measured and calculated excitation function of the  ${}^{60}\text{Ni}(p, \alpha){}^{57}\text{Co}$  process.

model calculations with properly chosen input parameters can reproduce not only the commonly occurring reactions, such as  $(p, n)$  and  $(p, \alpha)$ , but also the rather less-investigated process  $(p, \gamma)$ . A general comparison of the cross section at the maximum of the excitation function of each of the three reactions, namely,  $^{60}\text{Ni}(p, \gamma)^{61}\text{Cu}$ ,  $^{60}\text{Ni}(p, n)^{60}\text{Cu}$ , and  $^{60}\text{Ni}(p, \alpha)^{57}\text{Co}$ , amounting to 2, 320, and 85 mb, respectively, suggests that the  $(p, n)$  reaction is the most commonly occurring process and the  $(p, \gamma)$  reaction is rather weak. This is attributed to the higher probability of particle emission than  $\gamma$ -ray emission from the highly excited intermediate nucleus  $^{61}\text{Cu}$  formed in the interaction of a proton with the target nucleus  $^{60}\text{Ni}$ .

## V. CONCLUSION

The cross sections of the  $^{60}\text{Ni}(p, \gamma)^{61}\text{Cu}$  reaction determined in this paper by the activation technique were found to be comparable to those previously obtained via prompt  $\gamma$ -ray

counting, although in the 2.5–4-MeV region some discrepancy was observed. A theoretical calculation of this reaction using the nuclear model code TALYS showed that the measured excitation function is reproduced fairly well by a combination of compound and direct processes, except for the energy region below 4 MeV where some deviation occurs. A comparison of the cross sections at the maxima of the excitation functions of the three investigated proton-induced reactions on  $^{60}\text{Ni}$ , viz.  $(p, \gamma)$ ,  $(p, n)$ , and  $(p, \alpha)$ , suggests that the  $(p, \gamma)$  reaction is the weakest and the  $(p, n)$  reaction is the strongest.

## ACKNOWLEDGMENTS

M. S. Uddin thanks the Alexander von Humboldt Foundation of Germany for financial support to conduct this research work at FZ Jülich, Germany as well as at INST, Savar, Bangladesh. The authors thank the operational crews of the BC 1710 and the 3-MV tandem accelerator for performing irradiations.

- 
- [1] P. J. Daly, B. M. Seppelt, and P. F. D. Shaw, *Nucl. Phys. A* **119**, 673 (1968).
- [2] T. Sauter and F. Käppeler, *Phys. Rev. C* **55**, 3127 (1997).
- [3] B. Scholten, R. M. Lambrecht, M. Cogneau, H. Vera Ruiz, and S. M. Qaim, *Appl. Radiat. Isot.* **51**, 69 (1999).
- [4] EXFOR; Experimental Nuclear Reaction Data. Database version of October 6, 2015.
- [5] S. E. Woosley, W. D. Arnett, and D. D. Clayton, *Astrophys. J., Suppl. Ser.* **26**, 231 (1973).
- [6] D. D. Clayton and S. E. Woosley, *Rev. Mod. Phys.* **46**, 755 (1974).
- [7] D. M. Drake, S. L. Whetstone, and I. Halpern, *Nucl. Phys. A* **203**, 257 (1973).
- [8] G. A. Krivonosov, O. I. Ekchichev, B. A. Nemashkalo, V. E. Storizhko, and V. K. Chirt, *Izv. Rossiiskoi Akademii Nauk, Ser. Fiz.* **41**, 2196 (1977).
- [9] C. I. W. Tingwell, V. Y. Hansper, S. G. Tims, and A. F. Scott, *Nucl. Phys. A* **496**, 127 (1989).
- [10] A. Simon, A. Spyrou, T. Rauscher, C. Fröhlich, S. J. Quinn, A. Battaglia, A. Best, B. Bucher, M. Couder, P. A. Deyoung *et al.*, *Phys. Rev. C* **87**, 055802 (2013).
- [11] B. L. Cohen, *Phys. Rev.* **100**, 206 (1955).
- [12] S. Spellerberg, B. Scholten, I. Spahn, W. Bolten, M. Holzgreve, H. H. Coenen, and S. M. Qaim, *Appl. Radiat. Isot.* **104**, 106 (2015).
- [13] M. S. Uddin, A. K. Chakraborty, S. Spellerberg, M. A. Shariff, S. Das, M. A. Rashid, I. Spahn, and S. M. Qaim, *Radiochim. Acta* **104**, 305 (2016).
- [14] F. Tárkányi, K. Gul, A. Hermanne, M. G. Mustafa, F. M. Nortier, S. M. Qaim, B. Scholten, Y. Shubin, S. Takács, and Y. Zhuang, IAEA-TECDOC-1211 (2001), pp. 49–152.
- [15] C. F. Williamson, J. P. Boujot, and J. Picard, Tables of range and stopping power of chemical elements for charged particles of energies from 0.5 to 500 MeV, Report CEA-R 3042 (1966).
- [16] H. Piel, S. M. Qaim, and G. Stöcklin, *Radiochim. Acta* **57**, 1 (1992).
- [17] S. Sudár and S. M. Qaim, *Phys. Rev. C* **50**, 2408 (1994).
- [18] C. R. Brune and D. B. Sayre, *Nucl. Instrum. Methods Phys. Res., Sect. A* **698**, 49 (2013).
- [19] TENDL-2014: TALYS-based evaluated nuclear data library, A. J. Koning, D. Rochman, S. van der Marck, J. Kopecky, J. C. Sublet, S. Pomp, H. Sjostrand, R. Forrest, E. Bauge, H. Henriksson, O. Cabellos, S. Goriely, J. Leppanen, H. Leeb, A. Plompen, and R. Mills, [www.talys.eu/tendl-2014.html](http://www.talys.eu/tendl-2014.html).
- [20] S. Y. F. Chu, L. F. Ekström, and R. B. Firestone, Lund/LBNL Nuclear Data Service, Version 2.0, <http://nucleardata.nuclear.lu.se/nucleardata/toi/>.
- [21] M. N. Aslam and S. M. Qaim, *Appl. Radiat. Isot.* **89**, 65 (2014).
- [22] F. Szelecsényi, G. Blessing, and S. M. Qaim, *Appl. Radiat. Isot.* **44**, 575 (1993).
- [23] S. Tanaka, M. Furukawa, and M. Chiba, *J. Inorg. Nucl. Chem.* **34**, 2419 (1972).
- [24] S. Kaufman, *Phys. Rev.* **117**, 1532 (1960).
- [25] P. Reimer and S. M. Qaim, *Radiochim. Acta* **80**, 113 (1998).
- [26] A. J. Koning, S. Hilaire, and M. C. Duijvestijn, in *Proceedings of the International Conference on Nuclear Data for Science and Technology, April 22–27, 2007, Nice, France (2007)*, edited by O. Bersillon, F. Gunsing, E. Bauge, R. Jacquemin, and S. Leray (EDP Sciences, Les Ulis, France, 2008), pp. 211–214.
- [27] M. S. Uddin, S. Sudár, and S. M. Qaim, *Phys. Rev. C* **84**, 024605 (2011).
- [28] S. M. Qaim, S. Sudár, B. Scholten, A. J. Koning, and H. H. Coenen, *Appl. Radiat. Isot.* **85**, 101 (2014).
- [29] V. N. Levkovskij, Activation cross sections of nuclides of average masses ( $A = 40–100$ ) by protons and alpha particles with average energies ( $E = 10–50$  MeV), Inter-Vesi, Moscow, USSR (1991).
- [30] B. P. Singh, M. K. Sharma, M. M. Musthafa, H. D. Bhardwaj, and R. Prasad, *Nucl. Instrum. Methods Phys. Res., Sect. A* **562**, 717 (2006).